AD-A193 356 COMPUTATIONAL BOUNDARY CONDITIONS FOR THE INCOMPRESSIBLE NAVIER-STOKES EQ. (U) WISCONSIN UNIV-MADISON CENTER FOR MATHEMATICAL SCIENCES G A ACHE 1/1

UNCLASSIFIED OCT 87 CMS-TSR-88-12 DAAL03-87-K-0028 F/G 20/4 NL

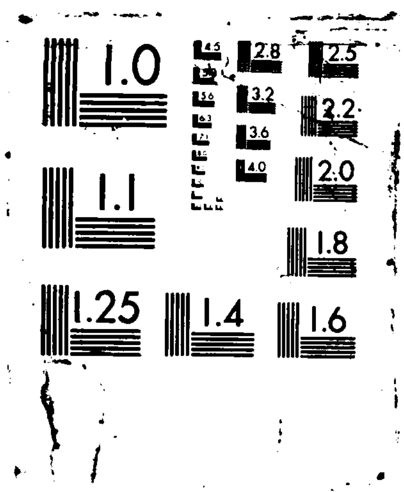
1.0
2.8
2.5
3.2
2.2
3.6
4.0
2.0
1.1
1.8
1.25
1.4
1.6

DTIC FILE COPY

AD-A193 356

CMS Technical Summary Report #88-12

COMPUTATIONAL BOUNDARY CONDITIONS FOR THE INCOMPRESSIBLE NAVIER-STOKES EQUATIONS IN CHANNELS AND PIPES

Gerardo A. Ache

UNIVERSITY OF WISCONSIN

CENTER FOR THE MATHEMATICAL SCIENCES

Center for the Mathematical Sciences
University of Wisconsin—Madison
610 Walnut Street
Madison, Wisconsin 53705

October 1987

(Received October 8, 1987)

Approved for public release
Distribution unlimited

Sponsored by

U. S. Army Research Office
P. O. Box 12211
Research Triangle Park
North Carolina 27709

UNIVERSITY OF WISCONSIN-MADISON
CENTER FOR THE MATHEMATICAL SCIENCES

COMPUTATIONAL BOUNDARY CONDITIONS FOR THE INCOMPRESSIBLE NAVIER-STOKES EQUATIONS IN CHANNELS AND PIPES

Gerardo A. Ache*

Technical Summary Report #88-12
October 1987

ABSTRACT

We derive inflow and outflow boundary conditions for the incompressible Navier-Stokes equations in cylindrical geometries. The purpose of these boundary conditions is to allow computations in a finite domain, that model flow in an unbounded domain, in a way that the accuracy of the finite difference solution is retained, making the computation more efficient. We use an approach similar to [9] to represent the solution asymptotically, far downstream and upstream, as a series expansion which involves eigenvalues and eigenfunctions. These eigensolutions satisfy certain systems of ordinary differential equations. The boundary conditions are represented by a family of differential operators in a way similar to what was done in [6] by Bayliss, Gunzberger and Turkel. To demonstrate the effectiveness of these boundary conditions we applied them in numerical computations of the incompressible Navier-Stokes equations in a channel with a step and in a pipe with a sudden enlargement of the cross section. To numerically solve the Navier-Stokes equations we used a second order accurate finite difference scheme ~~(Strikwerda [30])~~, also the boundary operators were approximated using second order accurate finite difference formulas. The numerical results show the effectiveness and the increase accuracy obtained by using the higher-order boundary conditions.

AMS(MOS) Subject Classifications: 35Q10, 35A40, 65N99

Key Words: Navier-Stokes, boundary conditions, differential operator, Poiseuille flow, Reynolds number, finite difference

*Facultad de Ciencias, Universidad Central de Venezuela-Caracas.
Mail address: Apdo 4311, Carmelitas, Caracas 1010, Venezuela.

Supported by the U. S. Army Research Office under Contract No. DAAL03-87-K-0028.

COMPUTATIONAL BOUNDARY CONDITIONS FOR THE INCOMPRESSIBLE NAVIER-STOKES EQUATIONS IN CHANNELS AND PIPES

Gerardo A. Ache*

1. Introduction

The development of boundary conditions for fluid flow in computational domains is an important subject in engineering applications, e.g. Engquist and Majda [12], Hedstrom [18], Bayliss and Turkel [6], Rudy and Strikwerda [29], Han and Innis [17]. In particular the determination of inflow and outflow boundary conditions for channel and cylindrical geometries is a very interesting problem in computational fluid dynamics. These boundary conditions are important since chosen properly they allow the size of the computational domain to be reduced and therefore cut down the time of computation. They also have a significant impact on the overall accuracy of the solution. In this paper we develop a class of inflow and outflow boundary conditions for the incompressible stationary Navier-Stokes equations. We consider that class of infinite domains which are combinations of cylinders or strips, (e.g. a channel with a step or a pipe with a sudden enlargement of the cross section), and for which conditions for flow into and out of the domain are needed in order to reduce the finite domain to a finite one.

*Facultad de Ciencias, Universidad Central de Venezuela-Caracas.
Mail address: Apdo 4311, Carmelitas, Caracas 1010, Venezuela.

Supported by the U. S. Army Research Office under Contract No. DAAL03-87-K-0028.

The unsteady flow of a viscous incompressible fluid satisfies the Navier-Stokes equations

$$\frac{\partial \mathbf{u}}{\partial t} + (\mathbf{u} \cdot \vec{\nabla})\mathbf{u} + \vec{\nabla} p - \nu \nabla^2 \mathbf{u} = \mathbf{f} \quad , \tag{1.1a}$$

$$\vec{\nabla} \cdot \mathbf{u} = 0 \quad , \tag{1.1b}$$

where $\mathbf{u}(\vec{x},t)$ is the velocity, $p(\vec{x},t)$ is the pressure, $\mathbf{f}(\vec{x},t)$ represents forces on the fluid, ν is the kinematic viscosity, $\vec{x}$ is in the domain Ω in R^N ($N = 2$ or 3) and $t \geq 0$. We here assume that the force $\mathbf{f}$ is derivable from a scalar potential P, i.e. $\mathbf{f} = -\nabla P$. Then we may rewrite the pressure as $p + P$. In addition to (1.1a), (1.1b) we may consider the boundary conditions

$$\mathbf{u} = \mathbf{g} \text{ on } \partial\Omega \quad , \tag{1.1c}$$

where $\mathbf{g}$ is required to satisfy

$$\int_{\partial\Omega} \mathbf{g} \cdot \vec{n} = 0 \quad , \tag{1.1d}$$

and the initial condition

$$\mathbf{u}(\vec{x},0) = \mathbf{h}(\vec{x}) \quad . \tag{1.1e}$$

The Navier-Stokes equations are important since they describe fluids such as air at low speeds, water, oil, etc. The mathematical aspects such as existence, uniqueness, and regularity of solutions related to these equations can be found in [24] and [32].

For the steady state Navier-Stokes equations in an infinite cylinder with cross section C there is a relatively simple solution called Poiseuille flow. If x_1 measures the distance along the axis, for this solution the velocity has the form $\mathbf{u}^{\infty}(\vec{x}) = (\hat{u}(x_2, x_3), 0, 0)$, and the pressure $p^{\infty} = -\bar{P}x_1$, with $\bar{P}$ a constant. Then $\hat{u}$ is solution of the equation

$$\nu\left(\frac{\partial^2 \hat{u}}{\partial x_2^2} + \frac{\partial^2 \hat{u}}{\partial x_3^2}\right) = -\bar{P} , \tag{1.2a}$$

and for which the flow condition

$$\int_C \hat{u} dx_2 dx_3 = Q > 0 , \tag{1.2b}$$

is satisfied.

In [1], [4], [20] and [21], are proven estimates which show that the difference $\mathbf{u}(\vec{x}) - \mathbf{u}^{\infty}(\vec{x})$ decays exponentially in the axial direction of a semi-infinite cylinder. This result is used to formulate our boundary conditions.

Since cylindrical geometries lead to Poiseuille flow at infinite distance, (inflow or outflow), one may impose at inflow or outflow the Poiseuille profile as a computational boundary condition. This is often done in computations involving the incompressible Navier-Stokes equations in channel and pipes, the resulting boundary conditions are of Dirichlet type. These conditions have been used for Navier-Stokes calculations and with different formulations, e.g. stream function-vorticity formulations or primitive variable formulations (e.g. [5], [11], [22], [25], [27]). Other type of computational boundary conditions are the specification of derivatives of the velocity or the stream function and vorticity at inflow or at outflow, (see [19], [23], [26]). For example, in [16] Greenspan performed Navier-Stokes calculations using Poiseuille flow as an inflow boundary condition, but at outflow he combined the vorticity and the stream function in a way that makes the pressure constant at the outflow boundary. He also carried out computations using Poiseuille flow at both boundary positions and he pointed out that both formulations were numerically equivalent. In [13] the effect of some downstream boundary conditions in a channel with a step are discussed for both the stationary and time dependent incompressible Navier-Stokes equations.

Since the Poiseuille profile occurs only in the limit at infinite distances, in order to construct better boundary conditions we may consider the asymptotic nature of the solution in the manner of Bramley and Dennis [9]. We assume that the solution can be regarded at large distances as Poiseuille flow plus a perturbation which decays exponentially fast. This perturbation is then expanded in terms of an eigenfunction series involving eigenvalues and eigenfunctions which satisfy certain system of ordinary differential equations [1], [8], [9], [10], [15] and [33]. Using this approach we may construct better boundary conditions by introducing an operator which annihilates the first few terms in the expansion. This method is closely related to that presented by Bayliss, Gunzburger, and Turkel [5] for the Helmholtz equation, where the concept of asymptotic expansion was applied to construct far-field boundary conditions, see also [7]. Similar to [5], the operators which define our boundary conditions are linear differential operators and they may involve derivatives of order greater than the order of the differential equations. These boundary conditions are different from the usual conditions used in incompressible Navier-Stokes calculations which involve only the variables and first derivatives. For linear systems of elliptic equations it is known (see [3]) that it is possible to prescribe boundary conditions defined in terms of linear differential operators involving derivatives higher than the order of the system and still have the problem be well-posed.

In [9] Bramley and Dennis formulated inflow and outflow boundary conditions in channel-like geometries which are similar to our first-order boundary conditions, but applied to the stream function formulation of the Navier-Stokes equations. They suggest that their conditions may be suitable for numerical work involving the incompressible Navier-Stokes equations.

To implement the boundary conditions we used finite difference formulas for the derivatives as efficiently as possible (these approximations are of the same order of accuracy as the order of the numerical scheme which is second order accurate (Strikwerda [30])). The numerical results, as discussed in section 4, show the effectiveness and the increase of accuracy obtained by using the higher order boundary conditions.

2. Development of Inflow and Outflow Boundary Conditions

Similar to Bramley and Dennis [9], we assume that the solution to the Navier-Stokes equations $(\mathbf{u}(\vec{x}), p(\vec{x}))$ can be represented asymptotically, far upstream or far downstream, in the form

$$\mathbf{u}(\vec{x}) = \mathbf{u}^{\infty}(\vec{y}) + \sum_{n} \mathbf{W}_n(\vec{y}) \exp(-\lambda_n x_1) \tag{2.1}$$

where $\vec{x} = (x_1, x_2, \cdots, x_N) = (x_1, \vec{y})$, and $\mathbf{u}^{\infty}(\vec{y})$ is the Poiseuille profile associated with the infinite cylinder. The set $\left\{\mathbf{W}_n(\vec{y}) \exp(-\lambda_n x_1)\right\}$ is assumed to be a complete set of eigenfunctions with $\left\{\mathbf{W}_n(\vec{y}), \lambda_n\right\}$ being solution to an eigenvalue problem which is described in §3. The eigenvalues λ_n satisfy,

$$|\lambda_n| \leq |\lambda_{n+1}| \quad \text{for } n = 1, 2, \cdots \ . \tag{2.2}$$

Eigenvalues with negative real part are associated to the asymptotic solution upstream (i.e. x_1 negative) and those with positive real part with the solution downstream (i.e. x_1 positive).

To construct an artificial boundary at $x_1 = d$ (inflow or outflow) we observe that from (2.1) we get the following relation,

$$\frac{\partial}{\partial x_1}(\mathbf{u} - \mathbf{u}^\infty) + \lambda_1(\mathbf{u} - \mathbf{u}^\infty)\Big|_{x_1=d} = O[\exp(-\lambda_2 d)] \quad , \tag{2.3}$$

i.e. the operator $\partial/\partial x_1 + \lambda_1$ annihilates the first term in the expansion (2.1). So we may define the following boundary condition at outflow or inflow, for d large,

$$\frac{\partial}{\partial x_1}(\mathbf{u} - \mathbf{u}^\infty) + \lambda_1(\mathbf{u} - \mathbf{u}^\infty)\Big|_{x_1=d} = 0 \quad . \tag{2.4}$$

A more accurate boundary condition is obtained by annihilating the first two terms in (2.1), and has an error of magnitude $O[\exp(-\lambda_3 d)]$. The operator is

$$(\frac{\partial}{\partial x_1} + \lambda_1)(\frac{\partial}{\partial x_1} + \lambda_2) \quad . \tag{2.5}$$

In case that λ_1 is complex with $\lambda_2 = \bar{\lambda}_1$ (2.5) becomes

$$\frac{\partial^2}{\partial x_1^2} + 2Re(\lambda_1)\frac{\partial}{\partial x_1} + |\lambda_1|^2 \quad . \tag{2.6}$$

To develop even more accurate conditions at the boundary, we consider the sequence of operators

$$B_m = \prod_{i=1}^{m}(\frac{\partial}{\partial x_1} + \lambda_i) \quad . \tag{2.7}$$

A straightforward calculation gives that $B_m(\mathbf{v}) = 0$, for any vector function $\mathbf{v}$ of the form

$$\mathbf{v}(\vec{x}) = \sum_{k=1}^{m} \mathbf{f}(\vec{y})\exp(-\lambda_k x_1) \quad . \tag{2.8}$$

Using the representation for $\mathbf{u}$ in (2.1) we obtain that

$$B_m(\mathbf{u} - \mathbf{u}^\infty)\Big|_{x_1=d} = O[\exp(-\lambda_{m+1} d)] \quad . \tag{2.9}$$

That is for any integer $m > 0$ the differential operator B_m annihilates the first m terms in the asymptotic expansion (2.1). Therefore we can use this family of operators as a way of matching asymptotically the solution up to the first m terms. We may therefore impose, at inflow or outflow, the following boundary conditions

$$B_m(\mathbf{u} - \mathbf{u}^\infty)\big|_{x_1 = d} = 0 \quad , \tag{2.10}$$

which is accurate at the boundary with an error of order $O\left[\exp(-\lambda_{m+1} d)\right]$. We may define a zero-order boundary condition replacing in (2.10) B_m by the identity operator. Then for $m = 0$, the boundary condition of this family is of a Dirichlet type which is the most common boundary condition used at inflow or outflow in engineering computations. However, one can expect a significant improvement in the efficiency of the computations by using the higher-order boundary conditions rather than the Dirichlet condition because of faster decrease of the error at the inflow or outflow boundary. The result will be a considerable gain in computer storage and running time as well, due to a reduction in the size of the computational domain. Notice that since the operators which define these boundary conditions involve higher-order derivatives we also can expect an increase of the difficulties in the implementation of these boundary conditions as the order increases. As we will show, these difficulties in the implementation are usually offset by the substantial increase in accuracy and efficiency.

3. The Eigenvalue Problems

The eigenpair $(\mathbf{W}_n(\vec{y}), \lambda_n)$ are obtained from an eigenvalue problem that results when we seek asymptotic solutions of the Navier-Stokes equations in the form

$$\mathbf{u}(\vec{x}) = \mathbf{u}^\infty(\vec{y}) - \mathbf{W}(\vec{y}) \exp(-\lambda x_1) \ , \tag{3.1a}$$

$$p(\vec{x}) = p^{\infty}(x_1) + R^{-1}q(\vec{y})\exp(-\lambda x_1) \ . \tag{3.1b}$$

For flow in a channel, neglecting nonlinear terms, these eigenvalue problems can be written as

$$\frac{d^2W_1}{dy^2} = -R\{\hat{u}(y)\lambda W_1 - \frac{d\hat{u}}{dy}W_2\} - \lambda\bar{q} - \lambda^2 W_1 \ , \tag{3.2a}$$

$$\frac{dW_2}{dy} = \lambda W_1 \ , \tag{3.2b}$$

$$\frac{d\bar{q}}{dy} = R\hat{u}(y)\lambda W_2 + \lambda^2 W_2 + \lambda\frac{dW_1}{dy} \ , \tag{3.2c}$$

with boundary conditions

$$W_1(\pm 1) = W_2(\pm 1) = 0 \quad . \tag{3.2d}$$

Similarly for axi-symmetric flow in a pipe

$$\frac{dW_1}{dr} = \lambda W_2 - \frac{W_1}{r} \ , \tag{3.3a}$$

$$\frac{d^2W_2}{dr^2} = R\{\frac{d\hat{u}}{dr}W_1 - \lambda\hat{u}(r)W_2\} - \frac{1}{r}\frac{dW_2}{dr} - \lambda^2 W_2 - \lambda\bar{q} \ , \tag{3.3b}$$

$$\frac{d\bar{q}}{dr} = R\hat{u}(r)\lambda W_1 + \lambda\frac{dW_2}{dr} + \lambda^2 W_1 \ , \tag{3.3c}$$

with boundary conditions,

$$W_1(0) = \frac{dW_2}{dr}(0) = 0 \ \text{ and } \ W_1(1) = W_2(1) = 0 \ , \tag{3.3d}$$

where $\hat{u}$ is the parabolic profile in Poiseuille flow, as defined in (1.2a), (1.2b) and $R = \frac{Q}{\nu}$ is the Reynolds number. Results concerning the numerical solution of these eigenvalue problems can be found in [1], [8], [9], [10], [15] and [33], for flow in a channel and in [1], for axi-symmetric flow in a pipe, also there are even and odd eigenvalues associated to the channel flow problem. In this paper we compute solutions of the Navier-Stokes equations, in a channel and a pipe, using inflow and outflow boundary conditions of the form (2.10), where the eigenvalues λ_i in B_m are determined from the eigenvalue problems (3.2) and (3.3) respectively.

4. Numerical Implementation

An important ingredient needed to test these boundary conditions is a numerical scheme to solve the Navier-Stokes equations. The method we used here is based on a second-order finite difference scheme to solve the Stokes and Navier-Stokes equations [29], [30]. This method deals with primitive variables formulation, i.e., it uses the velocity and the pressure as dependent variables. Then the laplacian and convection terms, given in conservative form, are discretized using standard centered difference formulas, while the pressure gradient and the continuity equation are discretized using regularized centered difference formulas [29], e.g.

$$\frac{\partial p}{\partial x} \approx \delta_{x0} p - \frac{1}{6} h^2 \delta_{x-} \delta_{x+}^2 p \quad , \tag{4.1a}$$

$$\frac{\partial p}{\partial y} \approx \delta_{y0} p - \frac{1}{6} h^2 \delta_{y-} \delta_{y+}^2 p \quad , \tag{4.1b}$$

$$\frac{\partial u_1}{\partial x} \approx \delta_{x0} u_1 - \frac{1}{6} h^2 \delta_{x+} \delta_{x-}^2 u_1 \quad , \tag{4.1c}$$

$$\frac{\partial u_2}{\partial y} \approx \delta_{y0} u_2 - \frac{1}{6} h^2 \delta_{y+} \delta_{y-}^2 u_2 \quad , \tag{4.1d}$$

where $(\delta_{x0}, \delta_{y0})$, $(\delta_{x-}, \delta_{y-})$, $(\delta_{x+}, \delta_{y+})$ are centered, backward, and forward differences in the x and y direction, respectively. Formulas (4.1) are used in the pressure gradient and the continuity equation. To determine the pressure on the boundaries cubic interpolation formulas are used, i.e.

$$p_{0,j} = 3(p_{1,j} - p_{2,j}) - p_{3,j} \quad , \tag{4.2a}$$

$$p_{i,0} = 3(p_{i,1} - p_{i,2}) - p_{i,3} \quad . \tag{4.2b}$$

To solve the resulting finite difference equations an extended S.O.R. iterative procedure [30] was used. This numerical method is very efficient and accurate. It has been used to compute flow in a spinning and coning cylinder [31].

To implement the boundary conditions, we construct numerical approximations to these derivatives of order $O(h^2)$, where h is the grid size in the axial direction. These approximations do not destroy the entire accuracy of the interior scheme. We provide the finite differences formulas used to approximate the differential operators for each boundary condition, e.g.

—First-order :

$$\left.\frac{\partial u}{\partial x_1}\right|_{N-1/2} = \frac{u_N - u_{N-1}}{h} + O(h^2) \quad . \tag{4.4}$$

—Second-order:

$$\left.\frac{\partial^2 u}{\partial x_1^2}\right|_{N-1} = \frac{u_N - 2u_{N-1} + u_{N-2}}{h^2} + O(h^2) \quad , \tag{4.5a}$$

$$\left.\frac{\partial u}{\partial x_1}\right|_{N-1} = \frac{u_N - u_{N-2}}{2h} + O(h^2) \quad . \tag{4.5b}$$

—Third-order :

$$\left.\frac{\partial^3 u}{\partial x_1^3}\right|_{N-3/2} = \frac{u_N - 3(u_{N-1} - u_{N-2}) - u_{N-3}}{h^3} + O(h^2) \quad , \tag{4.6a}$$

$$\left.\frac{\partial^2 u}{\partial x_1^2}\right|_{N-3/2} = \frac{u_N - (u_{N-1} + u_{N-2}) + u_{N-3}}{2h^2} + O(h^2) \quad , \tag{4.6b}$$

$$\left.\frac{\partial u}{\partial x_1}\right|_{N-3/2} = \frac{u_{N-1} - u_{N-2}}{h} + O(h^2) \quad . \tag{4.6c}$$

—Fourth-order :

$$\left.\frac{\partial^4 u}{\partial x_1^4}\right|_{N-2} = \frac{u_N - 4u_{N-1} + 6u_{N-2} - 4u_{N-3} + u_{N-4}}{h^4} + O(h^2) \quad , \tag{4.7a}$$

$$\left.\frac{\partial^3 u}{\partial x_1^3}\right|_{N-2} = \frac{u_N - 2(u_{N-1} - u_{N-3}) - u_{N-4}}{2h^3} + O(h^2) \quad , \tag{4.7b}$$

$$\left.\frac{\partial^2 u}{\partial x_1^2}\right|_{N-2} = \frac{u_{N-1} - 2u_{N-2} + u_{N-3}}{h^2} + O(h^2) \quad , \tag{4.7c}$$

$$\left.\frac{\partial u}{\partial x_1}\right|_{N-2} = \frac{u_{N-1} - u_{N-3}}{2h} + O(h^2) \quad . \tag{4.7d}$$

5. Test Problems

In order to test these boundary conditions we used two problems as test problems. The first problem corresponds to an incompressible viscous flow in a channel with a step (see Figure 1) which can be regarded as the union of two strips, one upstream of the form $R_1 = (\frac{1}{2}, 1) \times (-\infty, 0]$ and the strip downstream of the form $R_2 = (0,1) \times [0, \infty)$.

The Poiseuille solution associated with the infinite strip having the same cross section as R_1 is given by

$$\hat{u}(y) = 48(y - \frac{1}{2})(1 - y) \quad , \tag{5.1a}$$

$$p^{\infty}(x) = -\frac{96}{R}x + \bar{C}_1 \quad , \tag{5.1b}$$

where $\bar{C}_1$ is a constant.

Similarly the Poiseuille solution associated with the infinite strip with same cross section as R_2 is given by

$$\hat{u}(y) = 6y(1 - y) \quad , \tag{5.2a}$$

$$p^{\infty}(x) = -\frac{12}{R}x + \bar{C}_2 \quad . \tag{5.2b}$$

To solve the Navier-Stokes equations we imposed boundary conditions at inflow and outflow of the form (2.8), and the non-slip condition at the walls. The eigenvalues in the expansion (2.1) are obtained by solving the eigenvalue problems described in §3.

The second test problem consists of a pipe with a sudden enlargement on the cross section, the fluid motion is considered axi-symmetric. Computations are made only in half of the domain, so the computational domain is similar to that for the channel flow problem.

The Poiseuille solutions associated which each part of the domain are given by,

$$\hat{u}(r) = 4(1 - 4r^2) \quad , \tag{5.3a}$$

$$p^{\infty}(z) = -\frac{64}{R}z + \bar{C}_1 \ . \tag{5.3b}$$

for the pipe upstream, i.e. $R_1 = (0, \frac{1}{2}) \times (-\infty, 0)$ and

$$\hat{u}(r) = 1 - r^2 \quad , \tag{5.4a}$$

$$p^{\infty}(z) = -\frac{4}{R}z + \bar{C}_2 \ , \tag{5.4b}$$

for the pipe downstream, i.e. $R_2 = (0,1) \times [0,\infty)$.

These two problems have been the subject of many numerical studies in the last 20 years, e.g. [11], [16], [19], [22], [23], [25], [26], [27].

6. Numerical Results

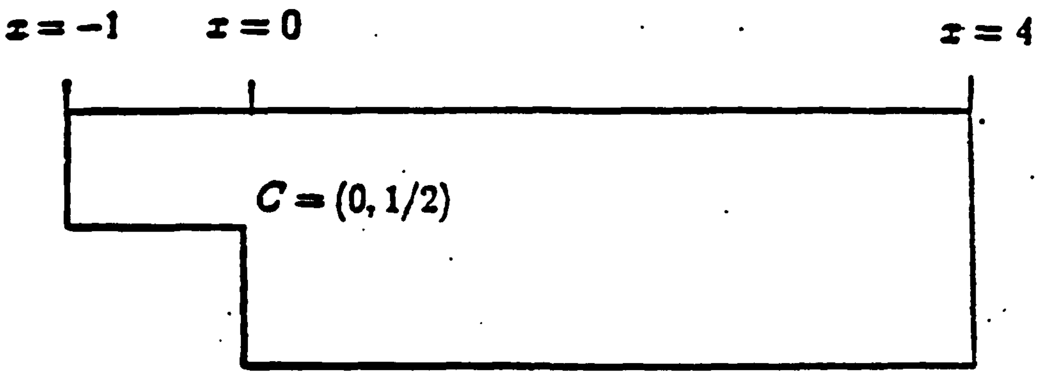

Figure 1: A Channel with a step.

We have done numerical computations which include the two test problems for flow in a channel and flow in a pipe. These two problems retain the full non-linear character of the Navier-Stokes equations. Boundary conditions of order 0, 1, 2, 3 and 4 have been applied at outflow for the channel flow problem and boundary conditions of order 0, 1 and 2 have been applied at outflow for the pipe flow problem. The specification of Poiseuille flow (zero-order boundary condition) was applied at inflow for both problems. The test positions where the computational boundaries were specified were at $x = d = -1$ (inflow) and $x = d = 4$ (outflow). The computations have been performed for Reynolds numbers R in the range $0 \leq R \leq 50$, and solutions were obtained in the largest domain ($d = 4$), using the grids 110×21, 140×29, and 170×35 at $R = 30$, 40, and 50, respectively, for the channel flow problem. Similarly for the pipe flow calculations the grid sizes were 50×21, 70×21, and 110×21 at $R = 10$, 20, and 30, respectively. The iterative procedure was stopped when the residuals of the difference satisfied a given tolerance of $.5 \times 10^{-5}$ in the largest domain and $.5 \times 10^{-4}$ for computations in the shorter domain (i.e. $d < 4$). All the computations were done on the VAX 11/780 at the Mathematics Research Center at the University of Wisconsin-Madison.

The numerical study included the following aspects related to the boundary conditions. For a fixed domain, we considered the effect of these boundary conditions as the Reynolds number was increased. For a fixed Reynolds number, we considered the effect of these boundary conditions as the domain was reduced.

In Figures 2.1a to 2.3b we display graphs corresponding to the velocity field at the center line of R_2, for the channel and pipe, downstream, i.e, at the line $\Gamma = \{(x, y)/y = \frac{1}{2}, a \leq x \leq d\}$, where a is greater than zero (i.e, away from the step). These graphs show how the solution is affected when boundary conditions of different orders are applied. In the channel flow problem at R equal to 30 Figures 2.1a to 2.1b show the velocity field corresponding to the domain at different distances downstream (i.e, d is 4 and d is 1.5), these solutions correspond to boundary conditions of order 0,2,3, and 4. Since at that Reynolds number the first and second eigenvalues in the expansion (2.1) are a complex conjugate pair (even) and the third and fourth eigenvalues are real (odd and even), see Table 1, it is not appropriate to use a first-order boundary condition. In Figure 2.1a we notice that the solutions for the different boundary conditions are close together, except near the outflow boundary where the solution corresponding to the zero-order boundary condition presents the largest deviation from solutions obtained using the higher-order conditions. As the domain is reduced from d of 4 to 1.5 the solution corresponding to the zero-order condition separates from the solutions corresponding to the higher-order condition, these solutions remaining close together. We computed the absolute and percentage errors for the difference between the solution in the largest domain and solutions in a shorter domain, for each boundary condition, these errors were measured using the discretized L_2-norm, i.e., if U_h^k is the numerical solution in the largest domain, corresponding to boundary condition of order k, and V_h^k is the numerical solution in a shorter domain, then the absolute and relative error are defined as $\triangle^k := \|U_h^k - V_h^k\|_2$ and $\triangle^k/\|U_h^k\|_2$ respectively, where $\|U_h\|_2 := h(\sum_j \sum_i U_{ij}^2)^{1/2}$, and the sum is taken over all the grid points. We have found that at R equal to 30, the numerical solution obtained using the zero-order condition in the domain with outflow test positions at d equal to 1.5 present percentage errors of about 12%, while for solutions corresponding to the higher-order condition these percentage errors were less than 1%.

At Reynolds number 40 and 50 the first two eigenvalues in (2.1) are real (odd and even) and the third eigenvalue is complex (even) and thus we applied boundary conditions of order $0, 1, 2$ and 4. We notice that at R equal to 40 the gap, near the outflow boundary, between the numerical solutions corresponding to the zero-order condition and solutions corresponding to the higher-order condition is bigger that for those at R equal to 30. For $d < 3$ a numerical solution using the first-order boundary condition could not be obtained, and for d equal to 1.5 solutions were obtained only for boundary conditions of order 2 and 4. For R equal to 50 and d equal to 4, solutions were obtained for all boundary conditions. At d equal to 3 solutions were obtained for the first, second and fourth order boundary conditions, at d equal to 2 solutions were obtained using the second and fourth order boundary condition and at d equal to 1.5 a solution was obtained only for the fourth-order boundary condition. For these Reynolds numbers the largest absolute and percentage errors correspond to numerical solutions obtained using the zero-order boundary condition, also the absolute and percentage errors for solutions corresponding to the higher-order condition become smaller as the Reynolds number is increased, that is due to the grid size being finer. These grid sizes were necessary in order to get a solution using the zero-order boundary condition. However, solutions on a coarser grid can be obtained using the higher-order boundary conditions. As we increased the Reynolds number from R equal to 50 to R equal to 60 we could not get a solution using the zero or first order condition on the coarser grid, however as the grid was refined a solution was obtained using the first-order condition but not the zero-order condition.

For the pipe flow problem we present the same type of results as for the channel flow problem. In this case the effect of using the zero-order boundary condition or a higher-order condition is more notable, notice also that the eigenvalues for this case are smaller in magnitude than those for the channel flow problem (Tables 1,2). For this problem we applied boundary conditions of order 0 and 1 at Reynolds numbers R equal to 10, 20 and boundary conditions of order 0, 1 and 2 at R equal to 30 , these conditions correspond to real eigenvalues in the expansion (2.1). Similar to the channel flow problem, we computed absolute and percentage errors for the different boundary conditions. In this case the percentage errors corresponding to the zero-order boundary condition, for the pipe flow problem, are much bigger than those for the channel flow problem (see Table 3). It is then possible to appreciate the effect of these boundary conditions in the stream function and pressure contour plots. In Figures 3.a to 3.d we present stream function and pressure contour plots for different boundary conditions at different test positions. Notice that near the outflow boundary in the pressure contour plots corresponding to the zero-order condition (Figures 3.a, 3.c) there are contours that can not be seen for the pressure contour plots corresponding to the higher-order condition. Similarly the stream function contour plots associated to the zero-order condition (Figures 3.a, 3.c) presents some oscillations near the outflow boundary while the stream function contour plots corresponding to the higher-order condition do not present those oscillations. These oscillations in the pressure and in the stream function contour plots are the result of the zero-order boundary condition being applied. Notice that in the stream function contour plots the oscillations are not as big as for the pressure contour plots, that is because we computed the stream function integrating the velocity, using the trapezoidal rule, and the integration acts to smooth the values.

7. The Pressure Corner Singularity

Analytically, it can be shown ([1], [2]) that for plane flow the pressure, near a re-entrant corner, behave as

$$p \approx A_1 r^{-0.456} + O(r^{-0.091}) \ , \tag{7.2}$$

where A_1 is a constant, and the pressure is given, near the corner, in polar coordinates, with the origin at the re-entrant corner.

Since the geometries considered in this paper, for the two test problems, present re-entrant corners and the pressure tends to be unbounded as the re-entrant corner is approached we need to provide, to the finite difference scheme finite pressure values at such corners, as efficient as possible, to evaluate the pressure gradient at adjacent grid points. In our situation, since the numerical scheme requires values of the pressure at the solid wall and since these values are computed using extrapolation formulas (as described in §4), we may compute the pressure at the corner in two different ways using such extrapolation formulas for each of the two directions. Assuming that the re-entrant corner is located at (x_0, y_0), we have

$$\begin{aligned} P_{c,x} &:= p(x_0, y_0) \\ &= 3(p(x_0 + h_x, y_0) - p(x_0 + 2h_x, y_0)) + p(x_0 + 3h_x, y_0) \ , \end{aligned} \tag{7.1a}$$

and

$$\begin{aligned} P_{c,y} &:= p(x_0, y_0) \\ &= 3(p(x_0, y_0 + h_y) - p(x_0, y_0 + 2h_y)) + p(x_0, y_0 + 3h_y) \ . \end{aligned} \tag{7.1b}$$

Here h_x, h_y are the grid sizes in the x and y directions respectively. Notice that since these values of $P_{c,x}$ and $P_{c,y}$ do not need to be equal it suggests that the pressure at a re-entrant corner may be regarded as a double valued function. Therefore to evaluate the pressure gradient at adjacent grid points we use $P_{c,x}$ to compute the approximation to $\partial p/\partial x$ at $(x_0 + h_x, y_0)$ and $P_{c,y}$ to compute the approximation to $\partial p/\partial y$ at $(x_0, y_0 + h_y)$.

The pressure strategy described above works well in computation at small and moderate Reynolds numbers and accurately models the pressure singularity, as it is shown in [1] and [2].

8. Conclusion

We have developed a family of local boundary conditions for the incompressible Navier-Stokes equations in channel and pipes. The boundary conditions are constructed using the fact that the solution possesses an asymptotic expansion of the form (2.1). Numerical results demonstrate the effectiveness of these boundary conditions. These results are summarized as follows:

1- For a given domain, a given grid size, and a given boundary condition, as the Reynolds number is increased a solution may or may not be obtained. In case the solution is not obtained either the finite difference solution does not exist or the iterative method fails to compute the solution. As the mesh is refined a solution may be obtained.

2- For a given domain, a given grid size, and a given Reynolds number, as the order of the boundary condition increases the accuracy of the finite difference solution improves.

3- For a given grid size, a given Reynolds number, and a given boundary condition, as the domain size increases the accuracy increases.

4- For a given domain, a given Reynolds number, and a given boundary condition, as the grid size decreases the accuracy increases.

These results demonstrate that the use of the higher-order boundary conditions can improve both the efficiency and the accuracy of fluid flow calculations.

Acknowledgements

I would like to thank Professor John C. Strikwerda for his valuable advice and the encouragement I have received during the preparation of this research.

This paper is a portion of my Ph.D dissertation, carried out at the University of Wisconsin-Madison. The final report was written while I was visiting the Center for the Mathematical Sciences, the University of Wisconsin-Madison.

This work was supported in part by the United States Army under Contract No. DAAG29-80-C-0041 and in part by Consejo de Desarrollo Cientifico y Humanistico, UCV, Caracas.

References

[1] Ache, G. A., "Incompressible Viscous Steady Flow in Channel and Pipes", Ph.D. dissertation, the University of Wisconsin-Madison (1985).

[2] Agmon, S., Douglis, A. and Nirenberg, L., " Estimates Near the Boundary for Solutions of Elliptic Partial Differential Equations Satisfying General Boundary Conditions, II", Comm. Pure App. Math. **17** (1964), 35–92.

[3] Amick, C. J., " Properties of Steady Navier-Stokes Solutions for Certain Unbounded Channels and Pipes", J. Nonl. Anal. Th. Appl. **6** (1978), 698–720.

[4] Aubert, X. and Deville, M., "Steady Viscous Flow by Compact Differences in Boundary Fitted Coordinates", J. Comput. Phys. **49** (1983), 490–522.

[5] Bayliss, A., Gunzburger, M. and Turkel, E., "Boundary Conditions for the Numerical Solution of Elliptic Equations in Exterior Regions", SIAM J. Appl. Math. **42** (1982), 430–451.

[6] Bayliss, A. and Turkel, E., "Radiation Boundary Conditions for Wave-like Equations", Comm. Pure Appl. Math. **33** (1980), 707–725.

[7] Bramley, J. S., "Note on the Calculation of Eigenvalues for Stationary Perturbation of Poiseuille Flow", J. Comput. Phys. **53** (1984), 524–529.

[8] Bramley, J. S. and Dennis, S. C. R., "The Calculation of Eigenvalues for the Stationary Perturbation of Poiseuille Flow", J. Comput. Phys. **47** (1982), 179–198.

[9] Bramley, J. S. and Dennis, S. C. R., "The Calculation of Eigenvalues for the Stationary Perturbation of Poiseuille Flow Using Initial Value Methods", J. Math. Anal. Appl. **101** (1984), 30-38.

[10] Dennis, S. C. R. and Smith, F. T., "Steady Flow Through a Channel with a Symmetric Constriction in the Form of a Step", Proc. Roy. Soc. Lond. **A 372** (1980), 393–414.

[12] Engquist, B. and Majda, A., "Absorbing Boundary Conditions for the Numerical Simulation of Waves", Math. Comp. **31** (1977), 629–651.

[13] Fix, G. and Gunzburger, M., "Downstream Boundary Conditions for Viscous Flow Problems", Comp. Math. Appl. **3** (1977), 53–63.

[14] Ghia, U., Ghia, K. N., Rubin, S. C. and Khosla, P. K., "Study of Incompressible Flow Separation Using Primitive Variables", Computers and Fluid **9** (1981). 123–142.

[15] Gillis, J. and Brandt, A., "The Numerical Integration of the Equation of Motions of a Viscous Fluid", Weizmann Institute, Report AF EOAR, SR-1 (1964). 63–73.

[16] Greenspan, D., "Numerical Studies of Steady Viscous Incompressible Flow in a Channel with a Step", J. Engng. Math. **3** (1969), 21–28.

[17] Han, T. Y. and Innis, G. E., "An Open Boundary Condition for Incompressible Stratified Flow", J. Comput. Phys. **49** (1983), 276–297.

[18] Hedstrom, G., "Non-Reflecting Boundary Conditions for Nonlinear Hyperbolic Systems", J. Comput. Phys. **30** (1979), 222–237.

[19] Hirt, C. W., "Simplified Solution Algorithms for Fluid Flow Problems", in Numerical Methods for Partial Differential Equations (S. Parter, ed.), Academic Press (1979), 193–211.

[20] Horgan, C. O., "Plane Entry Flow and Energy Estimates for the Navier-Stokes Equations", Arch. Rational Mech. Anal. **68** (1978), 359–381.

[21] Horgan, C. O. and Wheeler, L. T., "Spatial Decay Estimates for Navier-Stokes Equations with Applications to Entry Flow", SIAM J. Appl. Math. **35** (1978), 97–116.

[22] Kawaguti, M., "Numerical Solutions of the Navier-Stokes Equations for the Flow in a Channel with a Step", MRC Technical Summary Report #574 (1965).

[23] Kitchens, C. W., "Calculation of Low Reynolds Number Flow Past a Square Protuberance", A.I.A.A. J. **12** (1964), 1005–1007.

[24] Ladyzhenskaya, O. A., "The Mathematical Theory of Viscous Incompressible Flow", Gordon and Breach, New York (1969).

[25] Macagno, E. O. and Hung, T. K., "Computational and Experimental Study of a Captive Annular Eddy", J. Fluid Mech. **28** (1967), 43–64.

[26] Patera, A. T., "A Spectral Element Method for Fluid Dynamics: Laminar Flow in a Channel Expansion", J. Comput. Phys. **54** (1984), 468–488.

[27] Roache, P. J., "Computational Fluid Dynamics", Hermosa Pub., Albuquerque (1972).

[28] Roache, P. J. and Muller, T. J., "Numerical Solutions of Laminar Separated Flow", A.I.A.A. J. **8** (1970), 530–538.

[29] Rudy, D. H. and Strikwerda, J. C., "A Non-Reflecting Outflow Boundary Condition for Subsonic Navier-Stokes Calculations", J. Comput. Phys. **36** (1980), 55–70.

[30] Strikwerda, J. C., "Finite Difference Methods for the Incompressible Navier-Stokes Equations. A Survey", MRC Technical Summary Report #2584 (1983).

[31] Strikwerda, J. C., "Finite Difference Methods for the Stokes and and Navier-Stokes Equations", SIAM J. Sci. Statist. Comp. **5** (1984), 56–68.

[32] Strikwerda, J. C., "An Iterative Method for Solving Finite Difference Approximations to the Stokes Equations", SIAM J. Numer. Anal. **21** (1984), 447–458.

[33] Strikwerda, J. C., "A Numerical Study of Taylor-Vortex Flow", MRC Technical Summary Report #2808 (1985).

[34] Strikwerda, J. C. and Nagel, Y. M., "A Numerical Method for the Incompressible Navier-Stokes Equations in Three-Dimensional Cylindrical Geometry", to appear in J. Comput. Phys.

[35] Temam, R., "Navier-Stokes Equations and Nonlinear Functional Analysis", SIAM Regional Conference Series in Applied Mathematics **41** (1983).

[36] Wilson, S., "The Development of Poiseuille Flow", J. Fluid Mech. **38** (1968), 793–806.

TABLE 1

Eigenvalues from the expansion (2.1).for the channel flow problem

R	inflow λ_1	outflow λ_1	outflow λ_2	outflow λ_3
30	-6.33792	1.9842±i1.2012	2.48996	3.372034
40	-5.95994	1.86981	1.89935	2.1503±i1.1312
50	-5.69344	1.31807	1.49834	2.0832−i1.2186
60	-5.49035	0.95132	1.25008	1.9780−i1.2161

TABLE 2

Eigenvalues from the expansion (2.1), for the pipe flow problem

R	inflow λ_1	outflow λ_1	outflow λ_2
10	-11.2963±i2.1544	2.84871	4.2920+i1.42646
20	-9.89212	1.23859	3.9266±i0.7599
30	-9.38262	1.02639	2.83212

TABLE 3

Absolute and percentage errors betwwen the solution in the largest domain and solutions in a shorter domain (pipe flow)

R	d	B.C	$\triangle^k(^*)$	%	$\triangle^k(^{**})$	%
10	3	0	0.00048	1.28	0.00058	0.23
	2		0.00566	13.10	0.00594	2.72
	1.5		0.01779	38.72	0.01697	8.89
	3.0	1	0.00028	0.75	0.00059	0.23
	2.0		0.00081	1.87	0.00209	0.95
	1.5		0.00190	4.13	0.00438	2.29
20	3.0	0	0.01095	36.06	0.00869	3.92
	2.0		0.03650	115.63	0.02506	13.33
	3.0	1	0.00080	2.64	0.00108	0.49
30	3.0	0	0.03200	128.68	0.01989	9.83
	3.0	2	0.00001	0.05	0.00003	0.02

* The radial velocity component

** The axial velocity component

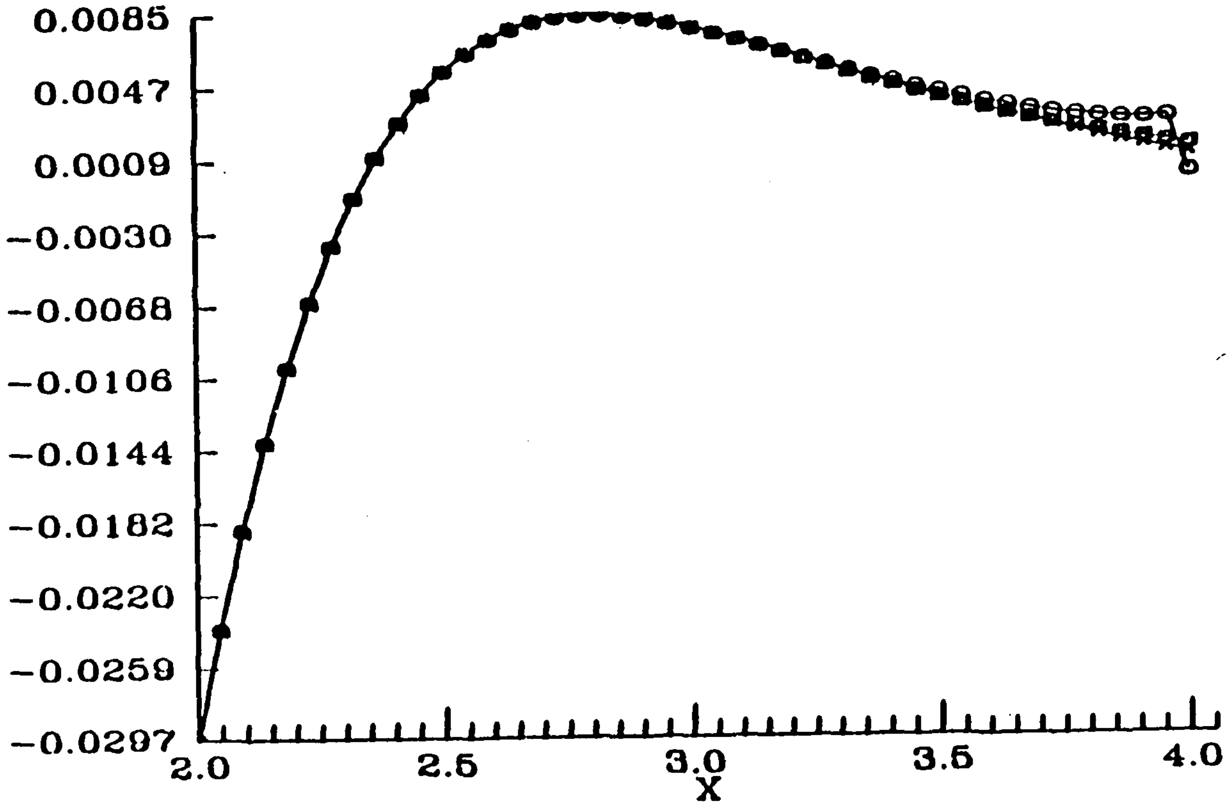

FIGURE 2.1a : Channel flow problem. The transverse velocity component on the centerline for $R = 30$ Boundary conditions of order 0,2,3 and 4 ($\circ, \times, \square, \Delta$).

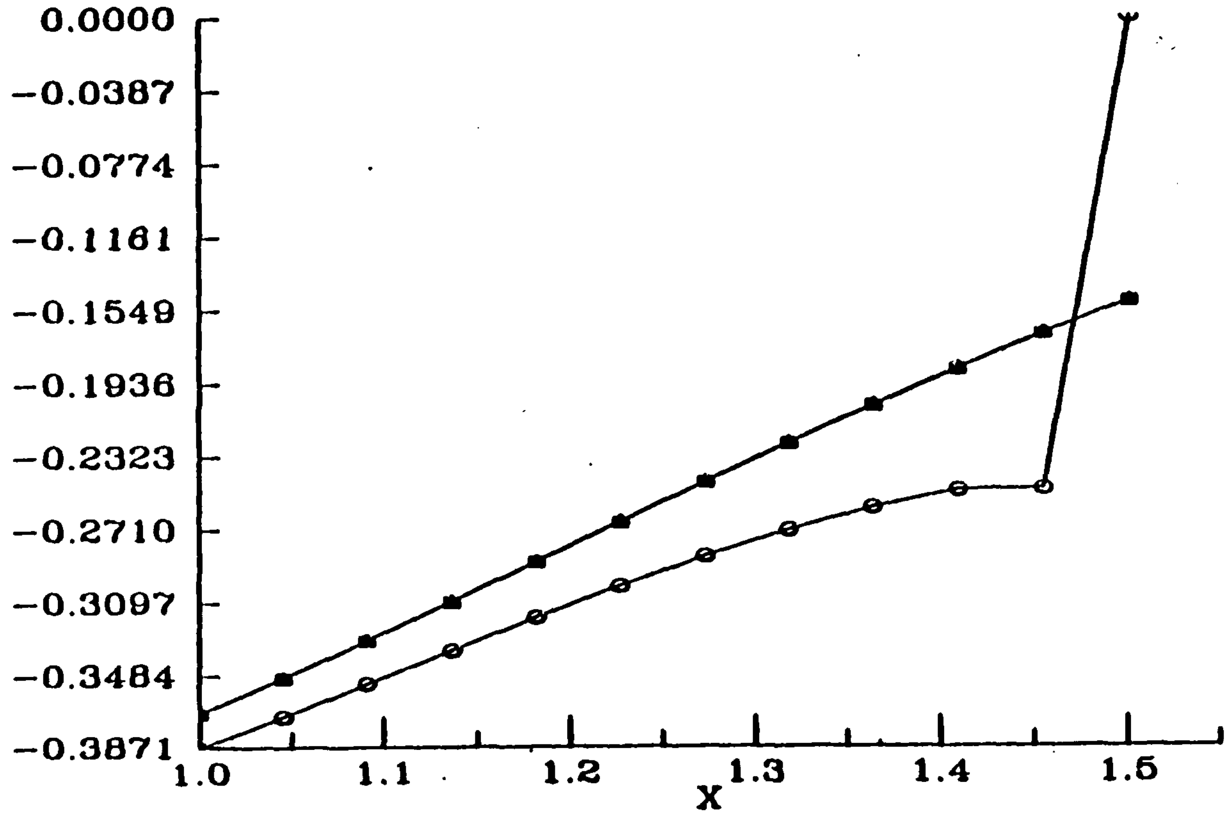

FIGURE 2.1b : Channel flow problem. The transverse velocity component on the centerline for $R = 30$ Boundary conditions of order 0,2,3 and 4 ($\circ, \times, \square, \triangle$).

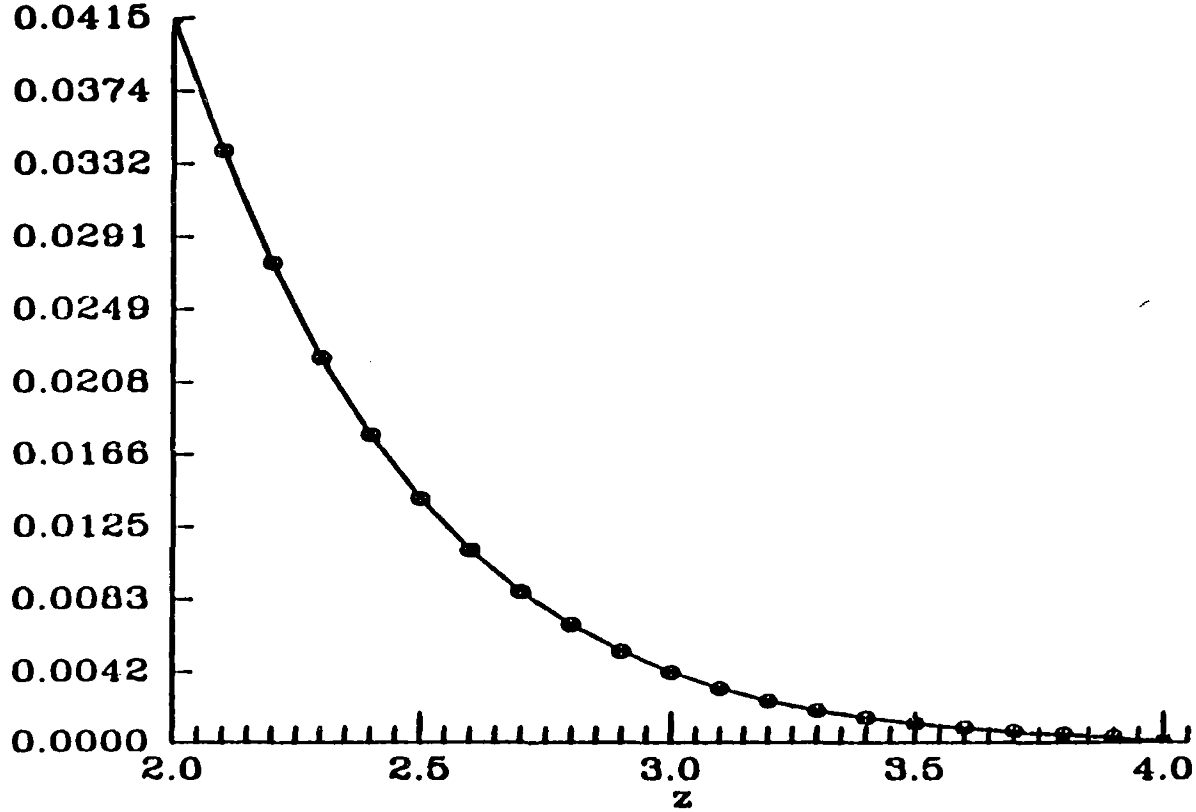

FIGURE 2.2a : Pipe flow problem. The radial velocity component on the centerline for $R = 10$ Boundary conditions of order 0 and 1 ($\circ, \times$).

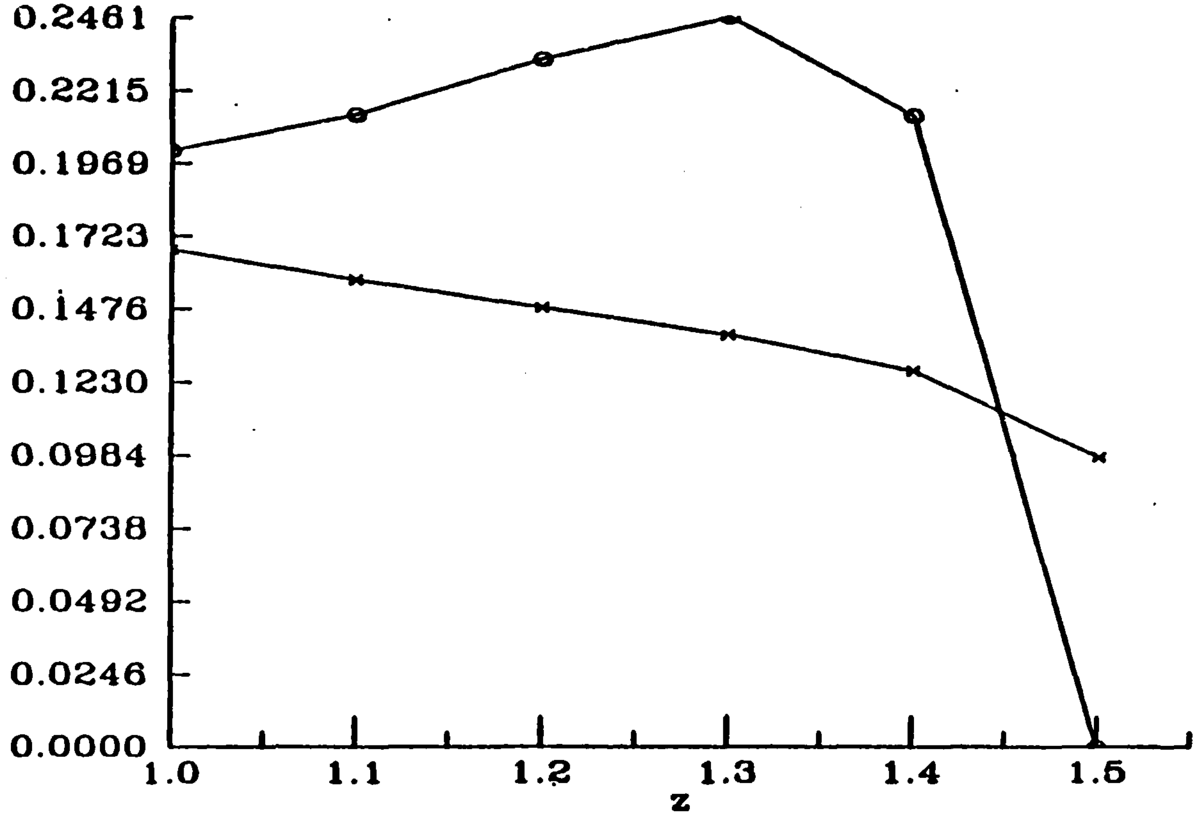

FIGURE 2.2b: Pipe flow problem. The radial velocity component on the centerline for $R = 10$ Boundary conditions of order 0 and 1 ($\circ, \times$).

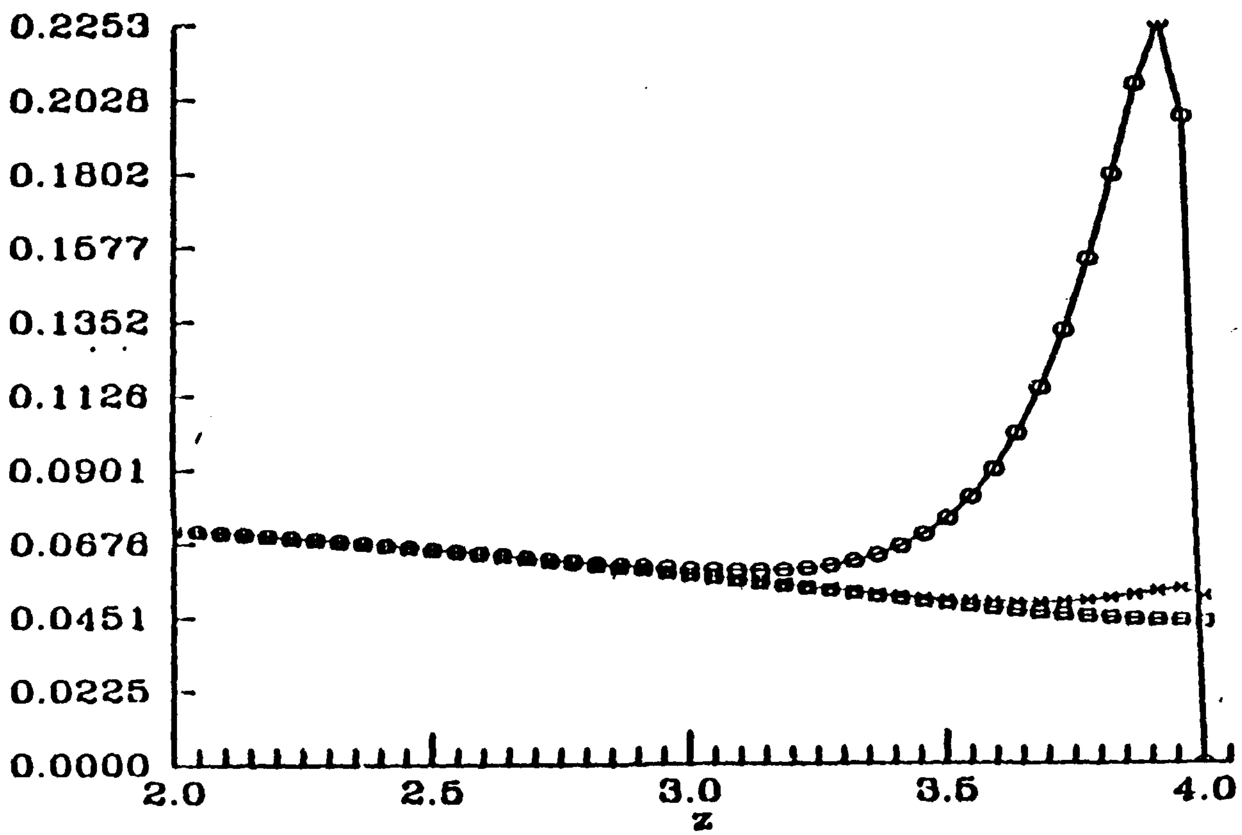

FIGURE 2.2c : Pipe flow problem. The radial velocity component on the centerline for $R = 30$ Boundary conditions of order 0,1 and 2 ($\circ, \times, \square$).

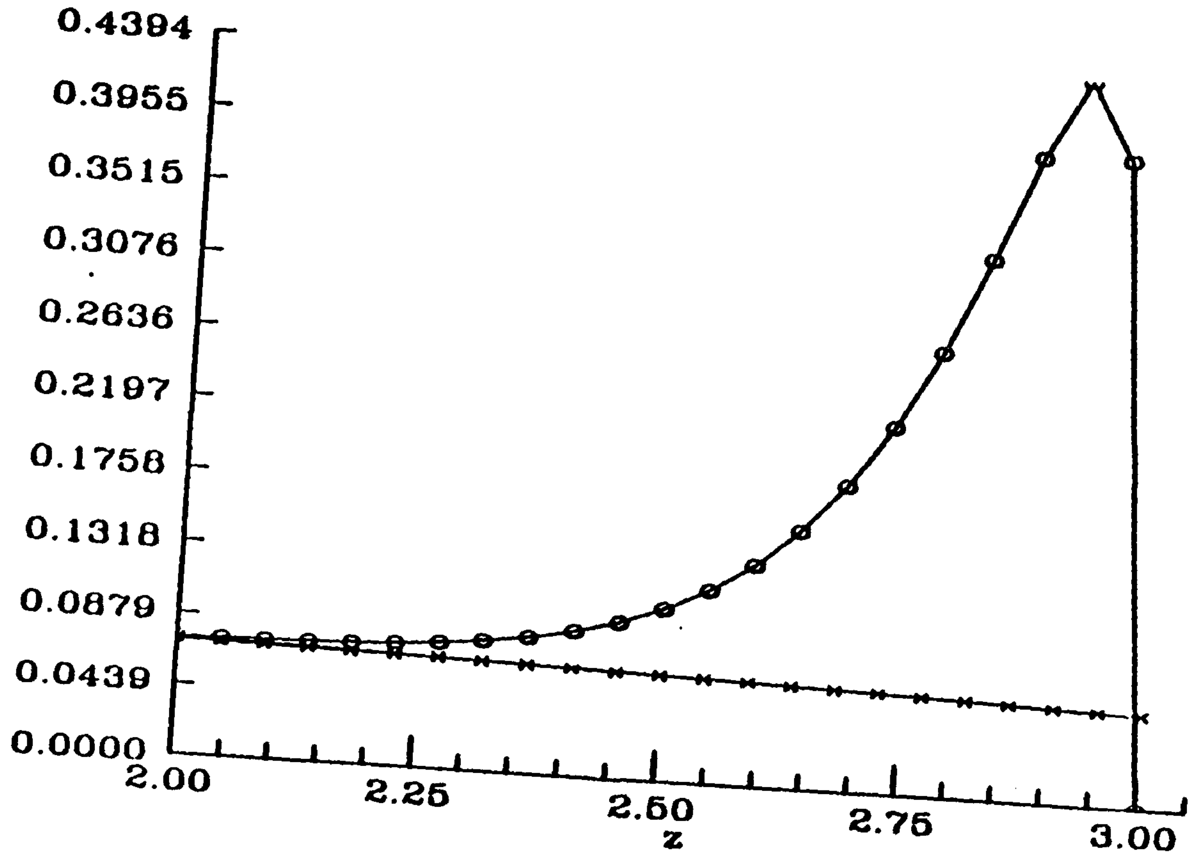

FIGURE 2.2d : Pipe flow problem. The radial velocity component on the centerline for $R = 30$ Boundary conditions of order 0 and 2 ($\circ, \times$).

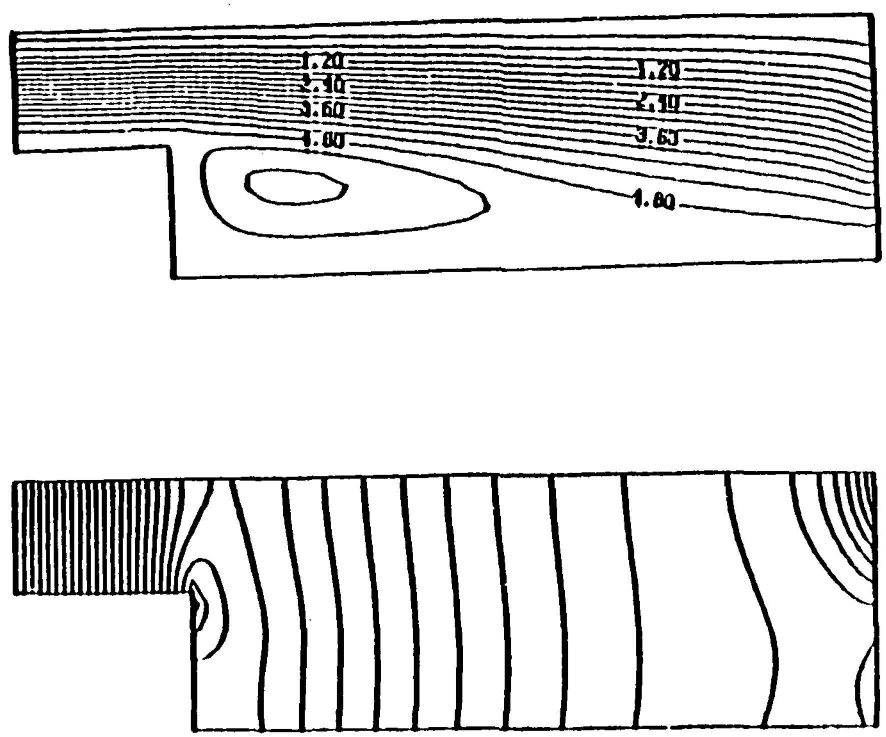

FIGURE 3.a : Pipe flow problem. Stream function and Pressure

$R = 30$. Boundary condition of order 0 . $d = 4$.

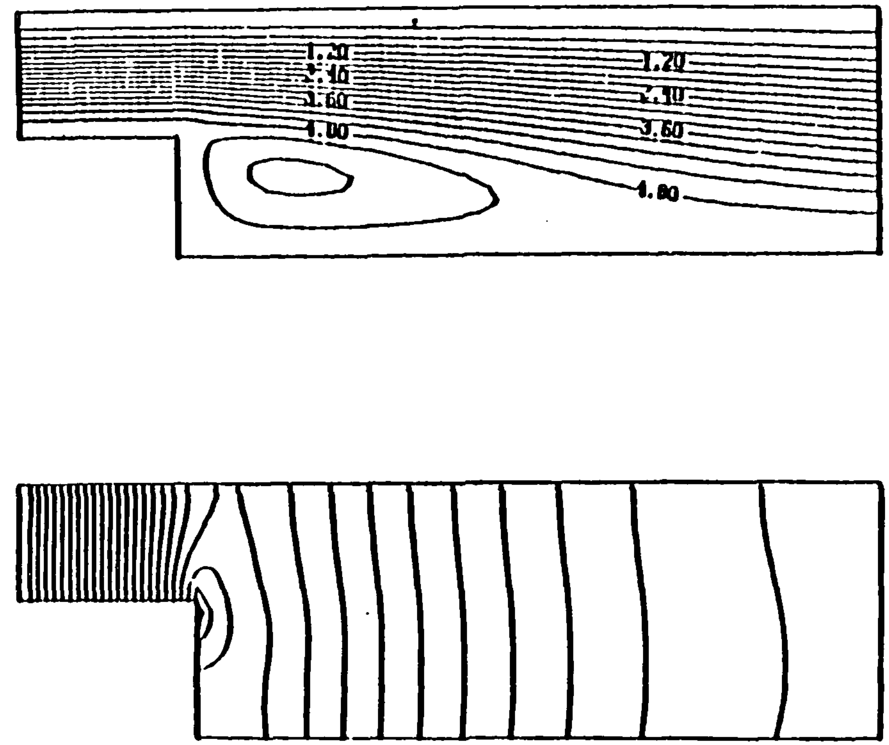

FIGURE **3.b : Pipe flow problem. Stream function and Pressure**

$R = 30$. Boundary condition of order 1 (or 2). $d = 4$.

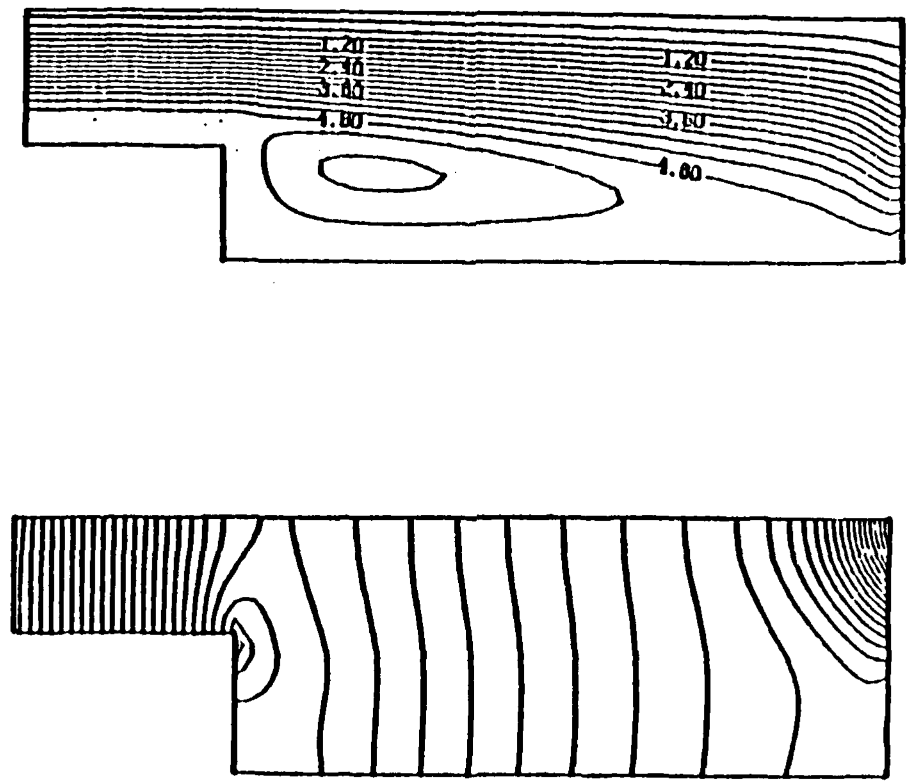

FIGURE 3.c : Pipe flow problem. Stream function and Pressure

$R = 30$. Boundary condition of order 0 . $d = 3$.

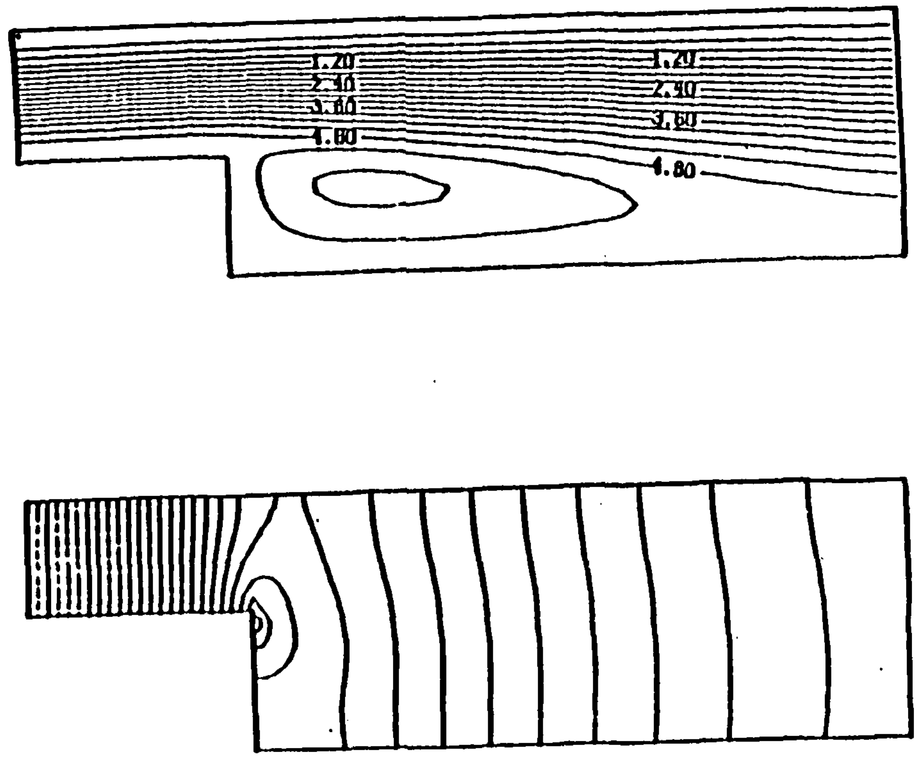

FIGURE 3.d : Pipe flow problem. Stream function and Pressure

$R = 30$. Boundary condition of order 2 . $d = 3$.

END
DATE
FILMED
DTIC
JULY 88